Colocated finite–volume schemes for large–eddy simulation on unstructured meshes

By S. Benhamadouche †, K. Mahesh ‡ AND G. Constantinescu

Code_Saturne ® is a finite-volume, unstructured-grid code developed at Électricité De France (*EDF*), which solves the Reynolds-averaged Navier-Stokes equations for incompressible flows. The code has been extensively benchmarked for a variety of industrial applications. The solver has been extended at *EDF* to solve large-eddy simulation equations, and we found that the numerical methods used in the base RANS code are not directly applicable to LES. This paper uses *Code_Saturne* to investigate the performance of several numerical schemes for LES of different academic and industrial flows. In particular, the conservation of global kinetic energy and robustness of several numerical schemes are compared and discussed. Finally, *Code_Saturne* with non-dissipative numerical methods is validated for the swirling flow in a coaxial geometry corresponding to the experiments of Sommerfeld & Qiu (1991). Also, the role of the subgrid-scale (SGS) model is investigated through simulations without a SGS model (coarse DNS), with a constant Smagorinsky model and with a dynamic Smagorinsky model.

Introduction

The objective of this work is to use an industrial code (*Code_Saturne* ®) developed at *EDF* to perform large-eddy simulation and to test several numerical schemes for LES. We adopt the point of view that LES requires non-diffusive numerical schemes, and therefore the numerical method used in the base RANS solver cannot be directly applied to LES. Recently Mahesh *et al.* (2001) developed an algorithm for unstructured grids that is discretely energy-conserving in the absence of time-splitting errors. Good prediction for a wide range of flows, including that in a Pratt & Whitney gas-turbine combustor, was reported. Also, an LES version has been developed at EDF with *Code_Saturne* (Benhamadouche *et al.* (2002)) and several tests have been done to improve the numerical schemes (Garibian *et al.* (2001)).

In this paper, we use *Code_Saturne* to evaluate the effect of the numerical method on discrete energy conservation. The effect of discrete time steps on both convection and pressure-gradient terms is considered. Results from the evaluation are used to decide upon a suitable scheme for LES using *Code_Saturne*, which is then applied to LES of the flow in a coaxial combustor geometry.

This paper is organized as follows. Section 1 describes the numerical schemes that are evaluated. The convection and pressure-gradient terms are discussed in subsections 1.1 and 1.2 respectively. Section 2 compares the different formulations for the Taylor problem and for isotropic turbulence. *Code_Saturne* is used to simulate the flow in a coaxial combustor geometry in section 3 and the results compared to experiment and results on the same grid using CDP, the unstructured solver developed by Mahesh *et al.* (2001).

† Electricité De France / UMIST (Manchester)
‡ University of Minnesota

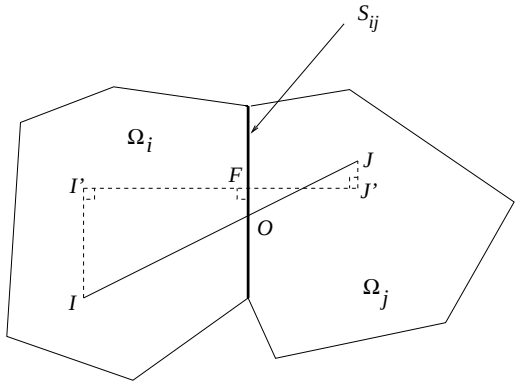

FIGURE 1. General view of a cell face

1. Numerical schemes

Code_Saturne solves the conservative form of the incompressible Navier Stokes equations (1.1). The code has the capability to use unstructured grids with cells of arbitrary shape.

$$\frac{\partial \mathbf{u}}{\partial t} + \mathrm{div}(\mathbf{u} \otimes \mathbf{u}) = -\mathbf{grad}(p) + \mathrm{div}\left[(\nu + \nu_t)\big(\mathbf{grad}(\mathbf{u}) + \mathbf{grad}^T(\mathbf{u})\big)\right] \tag{1.1}$$

$$\mathrm{div}(\mathbf{u}) = 0 \tag{1.2}$$

The following discussion focuses on two terms of the Navier-Stokes equations, the convection term and the pressure-gradient term.

1.1. *Convection term*

Two convection schemes have been tested. The first one is the default scheme used in *Code_Saturne* with RANS models and previous LES. It uses weighted coefficients and a reconstruction technique which is needed to account for the non-orthogonality which may occur at a cell face (figure 1). To evaluate the fluxes on the faces of a cell Ω_I, one has to compute the value of the velocity components at the center of the face F (cells Ω_I and Ω_J share face F in figure 1), $u_{i,F}$.

$$u_{i,F} = \frac{JO}{IJ}\, u_{i,I} + \frac{IO}{IJ}\, u_{i,J} + (\mathbf{grad}(u_i))_O.\overrightarrow{OF} \tag{1.3}$$

The main advantage of this scheme is that it maintains second-order accuracy in space on irregular Cartesian meshes and takes into account the geometrical non-orthogonality on unstructured meshes. However, the computation of $(\mathbf{grad}(u_i))_O$ in (1.3) is expensive if one wants to calculate this term implicitly at each time step.

The second scheme is easier to implement and has some interesting properties. It uses a symmetric formulation at the face, in which the velocity components at the face center are given by:

$$u_{i,F} = \frac{1}{2}u_{i,I} + \frac{1}{2}u_{i,J} \tag{1.4}$$

One can show, using discrete mass continuity, that the convection term which results from the discretization of the corresponding operator and use of (1.4) discretely conserves kinetic energy, provided that the transported velocity is estimated at $n+\frac{1}{2}$ with a Crank-Nicolson time-advancing scheme. This scheme, when tested for several canonical flows, shows good robustness. Note that in the algorithms where reconstruction is used for the convective term it is also used to calculate the quantities needed to estimate the other operators in the momentum equations (gradient, diffusion, ...). When the symmetric formulation for the convection term is used, no reconstruction is done for any of these fluxes. An intermediate scheme which uses the weighted coefficients (see (1.3)), but without the extrapolation with the gradient (the term $(\mathbf{grad}(u_i))_O.\overrightarrow{OF}$ in (1.3)), was found to be unstable and will not be discussed in detail.

1.2. *Pressure-gradient term*

Two algorithms have been also tested in *Code_Saturne* to insure the pressure/velocity coupling. The first algorithm is used by default in the code and employs Rhie & Chow's interpolation method. The pressure-velocity coupling is insured via the explicit pressure gradient at the previous time level in the momentum equations and by a projection method (SIMPLEC algorithm). The parameter α is set to 1 in (1.5), and $\mathbf{grad}_c$ and $\mathbf{grad}_f$ stand respectively for the cell and the face gradient in (1.5) and (1.6). This algorithm will be called **Alg1**.

$$\frac{\widetilde{\mathbf{u}}-\mathbf{u}^n}{\Delta t}+...=-\mathbf{grad}_c(p^n)+... \tag{1.5}$$

$$\mathrm{div}[\Delta t\ \mathbf{grad}_f(\delta p)]=\mathrm{div}\big(\widetilde{\mathbf{u}}+\alpha\ \Delta t\ \mathbf{grad}_c(p^n)-\alpha\ \Delta t\ \mathbf{grad}_f(p^n)\big) \tag{1.6}$$

The second algorithm (used also in CDP) does not take into account the explicit pressure gradient (cell gradient) in the momentum equations (see (1.7)). As the divergence of the pressure cell gradient may introduce odd-even decoupling on regular cartesian meshes, that is why this algorithm does not explicitly need the Rhie & Chow interpolation in the correction step (1.8). Odd-even decoupling will not occur as long as the Laplacian is coupling the cells (the same one used in the previous algorithm). This algorithm will be named **Alg2**.

$$\frac{\widetilde{\mathbf{u}}-\mathbf{u}^n}{\Delta t}+....=... \tag{1.7}$$

$$\mathrm{div}[\Delta t\ \mathbf{grad}_f(p^{n+1})]=\mathrm{div}(\widetilde{\mathbf{u}}) \tag{1.8}$$

Moreover, for the correction step, two approaches are possible to correct the velocity. If p stands either for δp or p^{n+1} (resulting from the discrete Poisson equation), one has to correct the velocity field $\widetilde{u}$ obtained from the predictor step :

$$\mathbf{u}^{n+1} = \widetilde{\mathbf{u}} - \Delta t\ \mathbf{grad}(p) \tag{1.9}$$

To compute $\mathbf{grad}(p)$, one can directly use Gauss' theorem to calculate the pressure gradient (in this case the correction step is $\mathbf{u}^{n+1} = \widetilde{\mathbf{u}} - \Delta t\ \mathbf{grad}_c p$), or a least-squares method to minimize the difference between estimating the normal gradient of the pressure at the faces directly and using the pressure gradient at the cell centers. In the latter case, one has to solve (1.10) locally at each cell, where the unknown is $\delta\mathbf{u}$, S the surface of the face between the neighbors I and J, and $\mathbf{n}$ the normal to the face. In this case, the velocity is corrected with $\mathbf{u}^{n+1} = \widetilde{\mathbf{u}} - \delta\mathbf{u}$.

$$\Sigma_J \Big(\delta\mathbf{u}(I).\mathbf{n}(F) - \Delta t\ \frac{\partial p}{\partial \mathbf{n}}(F) \Big) S^2 = 0 \tag{1.10}$$

2. Inviscid test cases

Several test cases have been considered. Inviscid flows have been chosen to check the conservation properties for kinetic energy and the robustness of the algorithms. The interest in inviscid flows is also motivated by the fact that high-Reynolds-number turbulent flows are close to this inviscid limit.

2.1. *Simulations on unstructured meshes with Cartesian topology*

In the case of uniform Cartesian grids, the two convection schemes give exactly the same result (because the faces are equidistant from the cell centers and the mesh is orthogonal). In addition, the two pressure-correction schemes described before are equivalent. Two test cases have been computed on Cartesian grids: 2D Taylor vortices and Homogeneous Isotropic Turbulence (HIT).

2.1.1. *Taylor vortices*

The fluid domain is a square whose side is 2π. The mesh contains 32×32 elements. Before analyzing the results obtained with the different algorithms proposed in this work, it is interesting to look at the performance of the usual algorithm used for RANS calculations. In this algorithm, the convective terms are evaluated using a blending of 20 % upwind and 80 % second-order-accurate central differences. This kind of scheme is typically used in RANS calculations but is not suitable for LES. Indeed, as one can clearly observe in figure 2, the effect of upwinding is to dramatically increase the numerical dissipation leading to a sharp decrease of the total kinetic energy. This result is obviously wrong, because for this inviscid periodic flow the total kinetic energy is supposed to be constant in time. Therefore, in the following, only fully-centered schemes will be considered.

Next, **Alg1** and **Alg2** are tested. Several time steps have been used and the total kinetic energy is plotted in figure 3 for a minimum ($\Delta t = 0.005$) and a maximum time step ($\Delta t = 0.1$). Figure 3 shows that the conservation of kinetic energy in both algorithms is not exact, due to time-splitting errors. **Alg2** is more dissipative than **Alg1** because the pressure is not included in the momentum equation during the prediction step. It is interesting to point out that simulations carried out with an explicit version of CDP showed better results for the conservation properties, comparable to those of **Alg1**. This is due to the fact that, because the convection term is treated explicitly, it contains the

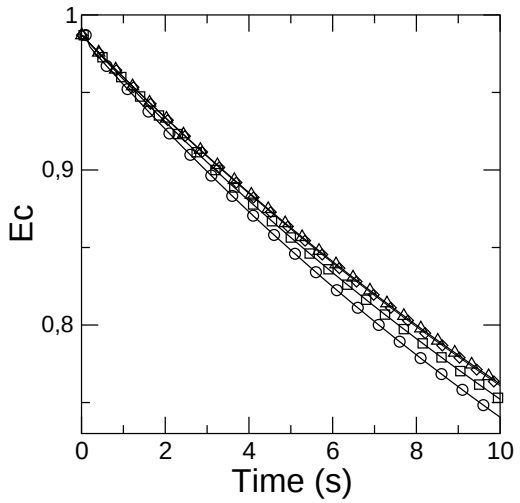

FIGURE 2. Taylor vortices - Evolution of kinetic energy with upwinding - $\Delta t = 0.1 : \circ$, $\Delta t = 0.05 : \square$, $\Delta t = 0.01 : \diamond$, $\Delta t = 0.005 : \triangle$

pressure from the previous corrector step, so in a sense the explicit version of CDP is closer to our **Alg1**. The other observation to be made is that in most LES simulations of complex flows (e.g. see section 3 and Mahesh et. al (2001)), the nondimensional time steps at which the calculations are run are considerably smaller than the time steps considered in these model problems; thus in most of these cases the time-stepping errors are not important even for **Alg2**.

Note that absolute conservation cannot be achieved in a colocated arrangement because of the Laplacian used in the Poisson equation. The mass flow contains the normal derivative (face gradient) of the corrected pressure (either δp or p^{n+1}) and the corrected velocity contains the cell gradient of this pressure. This is the case in both **Alg1** and **Alg2**. Figure 4 shows the time derivative of kinetic energy and the decay in energy due to the pressure gradient term for **Alg2**, with a very large time step $\Delta t = 0.1$. It shows that the term which is responsible for the loss in kinetic energy is the convection term, because the pressure term does not dissipate kinetic energy. Thus, the result of keeping the pressure gradient in the momentum equation even with the Rhie & Chow interpolation is to improve the conservation of the total kinetic energy. This is confirmed by the Homogeneous Isotropic Turbulence test case discussed next.

2.1.2. *Homogeneous Isotropic Turbulence*

A 32^3 mesh has been used in this case. The initial velocity field is generated using Comte-Bellot's experiment (AGARD (1998)). The viscosity is set to zero and the kinetic energy is computed at each time step. Figure 5 shows the decay of turbulent kinetic energy (which is the total kinetic energy in this case) using **Alg1** and **Alg2** and two different time steps. One can notice that the same behavior as in the previous test case is

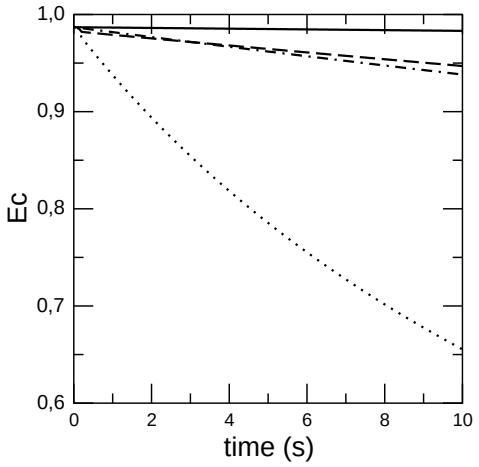

FIGURE 3. Taylor vortices - Evolution of kinetic energy - **Alg1** ($\Delta t = 0.1$) : dash, **Alg1**($\Delta t = 0.001$) : cont., **Alg2** ($\Delta t = 0.1$) : dot, **Alg2** ($\Delta t = 0.001$) : dash-dot.

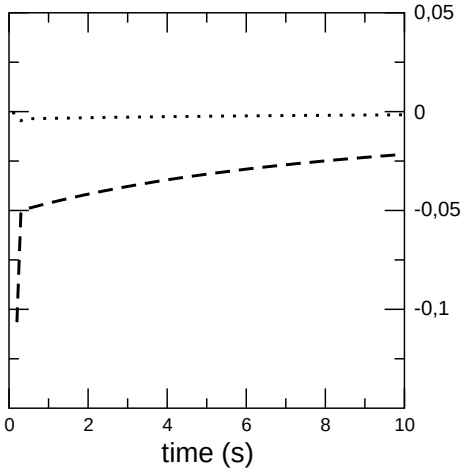

FIGURE 4. Taylor vortices - Contribution of the pressure gradient in the evolution of kinetic energy with **Alg2** and $\Delta t = 0.1$ - $\frac{\Delta E_c}{\Delta t}$: dash, $\mathbf{u}.\underline{\mathbf{grad}}(p)$: dot

observed; **Alg2** dissipates more energy than **Alg1**. The channel flow ($Re_\tau = 180$) test case has been computed with the two algorithms as well. The same behavior was observed.

2.2. *Simulations on fully-unstructured meshes*

The 2D flow corresponding to the Taylor problem has been simulated on a fully-unstructured mesh. This mesh is coarse and distorted and is representative of typical meshes used in industrial applications. In this case, both the effects of the convection scheme and of the pressure-correction algorithms described above can be tested.

In figures 6 and 7, all the cases have been run with the correction step based on the cell gradient. The effects of estimating the pressure gradient at cell centers using a least squares method will be discussed later. The simulations in figure 6 have been carried out with the reconstruction technique for the convection term - see (1.3). The calculations appear to be stable with both **Alg1** and **Alg2** when a relatively small time step is used. The numerical diffusion due to the projection step in this case is sufficient to dissipate the increase in the total kinetic energy. When the time step is decreased by a factor of 20, the calculations become unstable. This shows that for the inviscid case, the reconstruction method can entail an unstable computation.

Figure 7 shows the same case with smaller time steps, computed without any reconstruction technique - see eq. 1.4) - when the convection scheme is symmetric. The calculation is stable and visualization of the velocity field shows that the shape of the Taylor vortices is conserved in time. This proves that using this algorithm one can get robustness while maintaining accuracy, which is the main goal we want to achieve in simulations of complex flow of industrial interests using *Code_Saturne*. Note that the

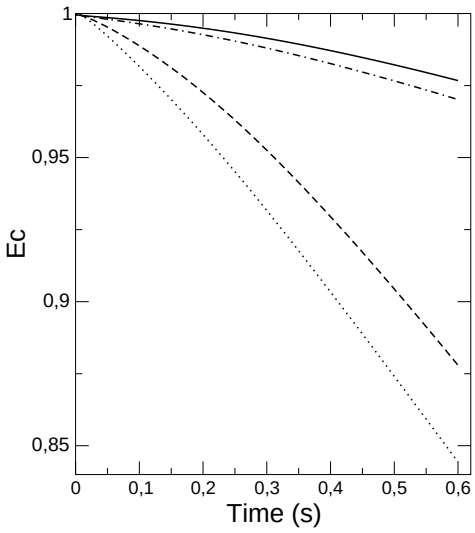

FIGURE 5. Homogemeous Isotropic Turbulence – Evolution of kinetic energy - **Alg1** ($\Delta t = 6 \times 10^{-3}$) : dash, **Alg1** ($\Delta t = 7.5 \times 10^{-4}$) : cont.,**Alg2** ($\Delta t = 6 \times 10^{-3}$) : dot, **Alg2** ($\Delta t = 7.5 \times 10^{-4}$) : dash-dot.

least-squares method used to reconstruct the pressure gradient at cell faces in the corrector step diverges, even when the symmetric formulation to compute the face velocity is used in the discretization of the convective terms. This seems to contradict the experience with CDP, which also uses this scheme and has shown good robustness when used to calculate a wide range of flows in complex geometries at high Reynolds numbers.

3. Turbulent cases – flow in a coaxial combustor geometry

The flow considered here consists of a primary jet issuing out of the core, and a swirling jet issuing out of an annular section around the core. These two streams of fluid mix as they enter the main coaxial combustor chamber. The flow is turbulent in both streams, with the Reynolds numbers around 26,000. As a result of the swirl, the streamlines diverge rapidly as they enter the main combustor chamber, and a recirculation region is set up. This is clearly visible in the contours of the instantaneous streamwise velocity component shown in figure 8. Sommerfeld & Qiu (1991) provide detailed measurements of this flow, including mean velocity components and their turbulent fluctuations at several stations inside the main combustor chamber. The inlet conditions are generated as explained in Pierce & Moin (2001) using a separate LES calculation. The inlet database, computational flow domain, mesh and the flow conditions are identical to those used in a simulation using CDP. The mesh in the present calculations contains 1.6 million cells.

The main purpose of this simulation is to show that the algorithms implemented in *Code_Saturne* can accurately simulate turbulence in complex configurations, are robust at high Reynolds numbers on fully unstructured meshes, and have an accuracy comparable to that of second-order-accurate structured codes and other unstructured solvers, in

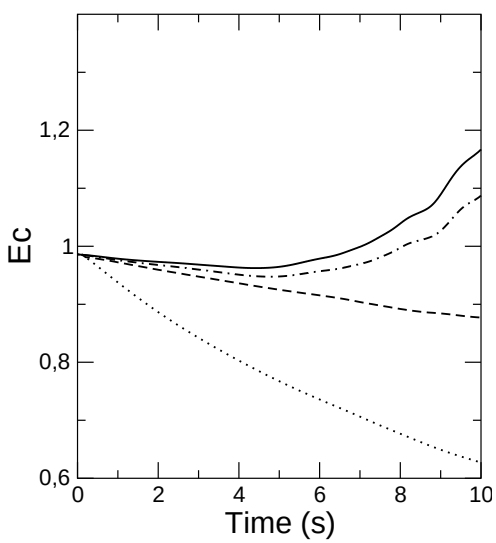

FIGURE 6. Evolution of kinetic energy - **Alg1** ($\Delta t = 0.1$) : dash, **Alg1** ($\Delta t = 0.005$) : cont., **Alg2** ($\Delta t = 0.1$) : dot, **Alg2** ($\Delta t = 0.005$) : dash-dot.

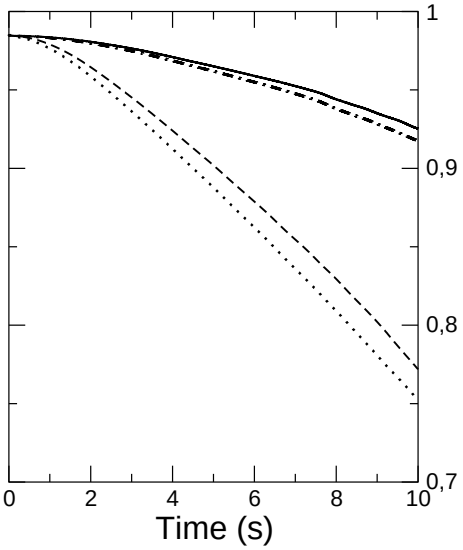

FIGURE 7. Evolution of kinetic energy - **Alg1** ($\Delta t = 0.005$) : dash, **Alg1** ($\Delta t = 6.2510^{-4}$) : cont., **Alg2** ($\Delta t = 0.005$) : dot, **Alg2** ($\Delta t = 6.2510^{-4}$) : dash-dot.

particular CDP, which uses an algorithm similar to **Alg2** and a symmetric formulation to evaluate the face velocity. In addition, sensitivity of the solution to the SGS model will be examined. Three simulations were performed using *Code_Saturne*, one in which a constant Smagorinsky SGS model with $C_s = 0.08$ was used, one in which no SGS model was used (coarse DNS) and, finally, one using a Smagorinsky SGS model with a coefficient calculated dynamically (we implemented the model described in Lilly (1992), with local averaging instead of the averaging in the homogeneous direction usually performed in structured codes). The algorithm employed in these simulations (**Alg1**) is the one that uses the Rhie & Chow interpolation and the symmetric formulation for the convection terms. No reconstruction technique was used.

A parallel version of *Code_Saturne* has been installed on an Origin 2000 machine and run on 32 processors to carry out these calculations.

The code was first run for approximately 100 nondimensional time units, defined with the mean inlet velocity in the core region and the annulus radius. Then statistics were computed over approximately the next 50 time units. Based on experience using CDP, these time intervals were found sufficient to eliminate the transients and to obtain converged statistics for this flow. As results using a second-order structured code and CDP were found to be very close (see Mahesh *et al.* 2001), we decided to plot only the experimental data, the results obtained with CDP, and the results of the three simulations performed with *Code_Saturne*. Figures 9, 10, 11, 12, 13 and 14 show, respectively, the mean

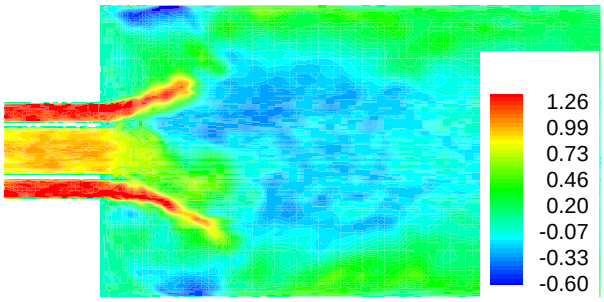

FIGURE 8. Instantaneous axial velocity with the dynamic model in *Code_Saturne* - Sommerfeld case

axial velocity, the mean fluctuations in the streamwise direction, the mean azimuthal velocity, the mean fluctuations in the azimuthal direction, the mean radial velocity, and the mean fluctuations in the radial direction.

Two-dimensional contour plots of the instantaneous and mean streamwise velocity (not shown) clearly show that in the simulation using the constant-coefficient Smagorinsky model the size of the recirculation bubble is not predicted correctly: the reattachment length of the detached shear layers is about 50% higher than that obtained from the experimental data or from the results obtained using CDP. This can be also inferred by comparing the location of the zero-velocity contour from the line plots of the streamwise velocity shown at different stations inside the main combustor chamber in figure 9. The other profiles also show a very poor level of quantitative prediction of the experimental measurements in contrast to the results using CDP.

As the prediction of this flow with CDP was shown to be very successful and the numerical methods used in the two codes are fairly similar, we suspected that the SGS model was responsible for the poor level of agreement with the experiment shown by the first calculation with *Code_Saturne*. Next we run a simulation without any SGS model (coarse DNS). This gave much better results, but a small overestimation of the recirculation zone compared to the experiment can still be observed from the line plots in figure 9. The other profiles also show a clear improvement in the prediction of the other velocity components and their turbulent fluctuations.

Finally, a calculation using a dynamic Smagorinsky model was run. Though the results show good agreement between CDP and this simulation for global quantities such as the size of the main recirculation region and the reattachment length on the lateral walls of the combustor, small differences remain when we compare the velocity statistics. Though some profiles obtained from the calculation with *Code_Saturne* are closer to the experimental data, on average CDP does a better job in predicting the flow, especially for the turbulent fluctuations. The differences between CDP and *Code_Saturne* results can be due to the different algorithms (CDP uses **Alg2** for the pressure correction) and to the somewhat different implementation of the dynamic model (explicit filtering).

4. Conclusions

Code_Saturne is an unstructured code, developed at *EDF*, which has been extensively validated using RANS models ($k-\varepsilon$ and *RSM* models). These turbulence models do

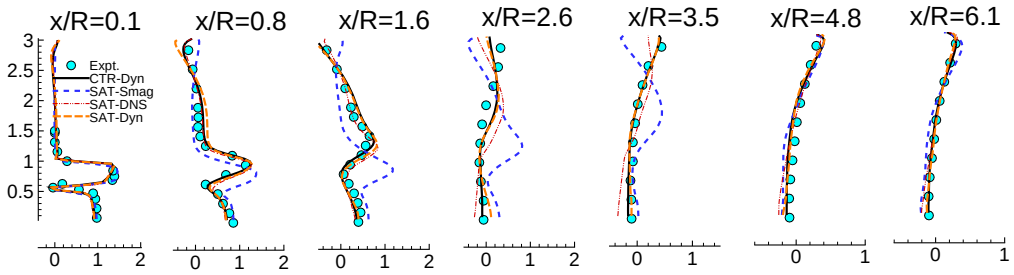

FIGURE 9. Mean axial velocity - Sommerfeld case

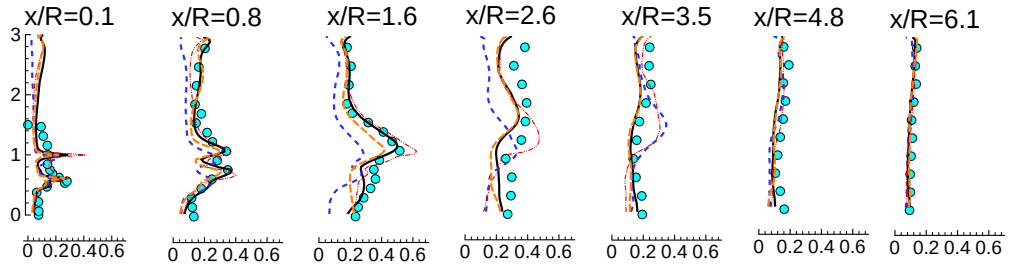

FIGURE 10. Mean axial fluctuations - Sommerfeld case

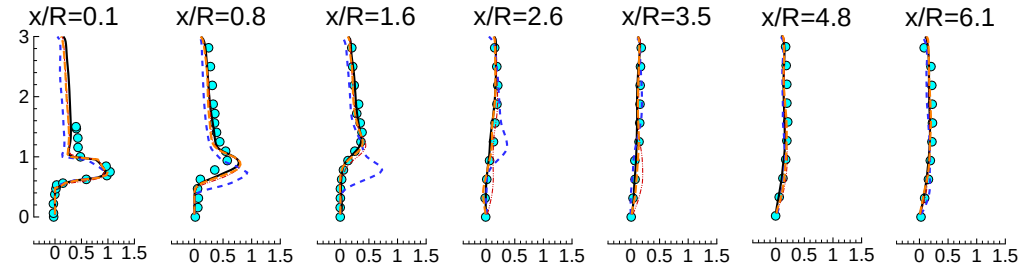

FIGURE 11. Mean tangential velocity - Sommerfeld case

not require strictly non-dissipative schemes. We extended *Code_Saturne* to solve the LES equations and noted that the numerical scheme must be non-dissipative. The use of non-dissipative schemes for high-Reynolds-number simulations is challenging because of the robustness problems. The proper way to address these problems is to try to insure conservation of kinetic energy, in a discrete sense, as accurately as possible. Several schemes have been tested in the present work, and we have shown that the usual Rhie & Chow interpolation for the pressure-gradient term is fairly acceptable for complex applications when only the mean quantities and Reynolds stresses are important. The convection term is more important; for fully-unstructured meshes, it has been shown that the use of the symmetric formulation for the convection term is more stable, as one can prove that the convection terms can be discretized in a way that fully conserves kinetic energy if the time-splitting errors are negligible. This study converged to a non-dissipative algorithm which was implemented in *Code_Saturne* and validated for several canonical flows as well as more complex turbulent flows. Future work will consist in applying this algorithm to simulate other complex flows of interest to *EDF*.

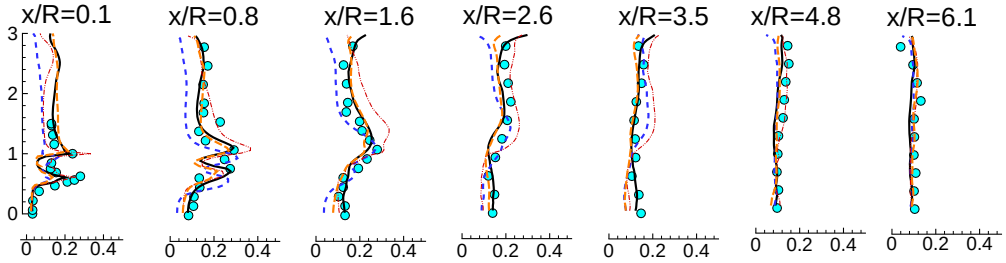

FIGURE 12. Mean tangential fluctuations - Sommerfeld case

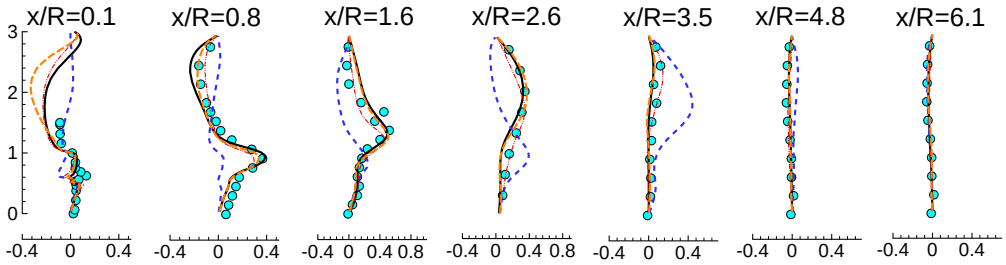

FIGURE 13. Mean radial velocity - Sommerfeld case

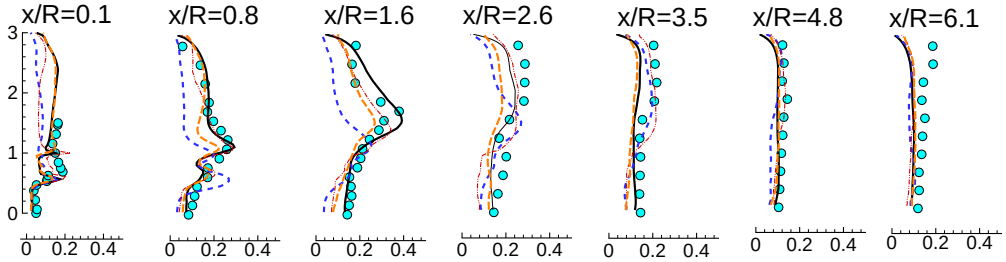

FIGURE 14. Mean radial fluctuations - Sommerfeld case

REFERENCES

ADVISORY GROUP FOR AEROSPACE RESEARCH AND DEVELOPMENT 1998 A selection of test cases for the validation of large-eddy simulation of turbulent flows. AGARD Advisory Rept. AR-345, North Atlantic Treaty Organization.

BENHAMADOUCHE, S. & LAURENCE, D. 2002 LES, COARSE LES, and transient RANS comparisons on the flow across a tube bundle. *5th International Symposium on Engineering Turbulence Modelling and Measurements Mallorca, Spain, 16-18 September 2002* (W. Rodi and N. Fueyo, eds.), Elsevier.

GARIBIAN, V., BENHAMADOUCHE, S. & LAURENCE, D. 2001 Schémas numériques conservant l'énergie cinétique avec une discrétisation colocalisée - Application à la Simulation des Grandes Échelles (LES). EDF report, HI-83/01/29.

LILLY, D. K. 1992 A proposed modification of the Germano subgrid-scale closure method. *Phys. Fluids. A* **4**, 633-635.

MAHESH, K., CONSTANTINESCU, G. & MOIN, P. 2000 Large Eddy Simulation of gas

turbine combustors. *Annual Research Briefs*, Center for Turbulence Research, NASA Ames/Stanford Univ., 219-229.

Mahesh, K., Constantinescu, G., Apte S., Iaccarino, G. & Moin, P. 2001 Large Eddy Simulation of gas turbine combustors. *Annual Research Briefs*, Center for Turbulence Research, NASA Ames/Stanford Univ., 3-19.

Pierce, C. D. & Moin, P. 1998 Method for generating equilibrium swirling inflow conditions. *AIAA Journal* **36**, 1325-1330.

Pierce, C.D. & Moin, P. 2001 Progress variable approach for large eddy simulation of turbulent combustion. *Report TF-80*, Flow Physics and Computation Division, Mechanical Engineering Dept., Stanford University, Stanford, California.

Sommerfeld, M. & Qiu, H.H. 1991 Detailed measurements in a swirling particulate two-phase flow by a phase-Doppler anemometer *Int. J. Heat Fluid Flow* **12**, 20-28.